Science of the Total Environment 769 (2021) 144558

Contents lists available at ScienceDirect

Science of the Total Environment

journal homepage: www.elsevier.com/locate/scitotenv

A highly agricultural river network in Jurong Reservoir watershed as significant CO_2 and CH_4 sources

Qitao Xiao [a], Zhenghua Hu [b,*], Cheng Hu [c], A.R.M. Towfiqul Islam [d], Hang Bian [b], Shutao Chen [b], Chao Liu [b], Xuhui Lee [e]

[a] Key Laboratory of Watershed Geographic Sciences, Nanjing Institute of Geography and Limnology, Chinese Academy of Sciences, Nanjing 210008, China
[b] Collaborative Innovation Center on Forecast and Evaluation of Meteorological Disasters, School of Applied Meteorology, Nanjing University of Information Science and Technology, Nanjing 210044, China
[c] College of Biology and the Environment, Joint Center for Sustainable Forestry in Southern China, Nanjing Forestry University, Nanjing 210037, China
[d] Department of Disaster Management, Begum Rokeya University, Rangpur 5400, Bangladesh
[e] School of the Environment, Yale University, New Haven, CT 06511, USA

HIGHLIGHTS

- The CO_2 and CH_4 dynamics varied between and within freshwaters.
- Fertilizer N input can stimulate aquatic CO_2 and CH_4 production and emission.
- The CO_2 and CH_4 saturations in river network were negatively correlated with DO.
- River network acted as significant sources of atmospheric CO_2 and CH_4.
- About 6% of net primary production was lost as aquatic carbon emission.

GRAPHICAL ABSTRACT

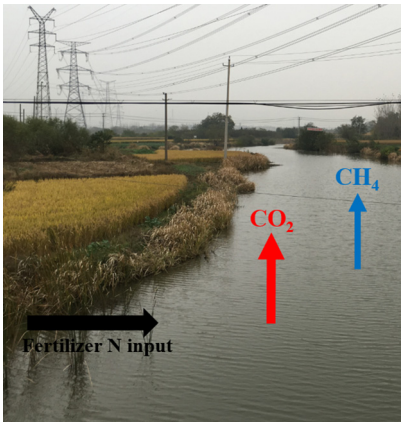

ARTICLE INFO

Article history:
Received 14 September 2020
Received in revised form 9 November 2020
Accepted 13 December 2020
Available online 17 January 2021

Editor: Ashanta Goonetilleke

Keywords:
Agricultural watershed
N loading
River network
CO_2 and CH_4 dynamics
Emission flux

ABSTRACT

Freshwaters are receiving growing concerns on atmospheric carbon dioxide (CO_2) and methane (CH_4) budget; however, little is known about the anthropogenic sources of CO_2 and CH_4 from river network in agricultural-dominated watersheds. Here, we chose such a typical watershed and measured surface dissolved CO_2 and CH_4 concentrations over 2 years (2015–2017) in Jurong Reservoir watershed for different freshwater types (river network, ponds, reservoir, and ditches), which located in Eastern China and were impacted by agriculture with high fertilizer N application. Results showed that significantly higher gas concentrations occurred in river network (CO_2: 112 ± 36 μmol L^{-1}; CH_4: 509 ± 341 nmol L^{-1}) with high nutrient concentrations. Dissolved CO_2 and CH_4 concentrations were supersaturated in all of the freshwater types with peak saturation ratios generally occurring in river network. Temporal variations in the gas saturations were positively correlated with water temperature. The saturations of CO_2 and CH_4 were positively correlated with each other in river network, and both of these saturations were also positively correlated with nutrient loadings, and negatively correlated with dissolved oxygen concentration. The highly agricultural river network acted as significant CO_2 and CH_4 sources with estimated emission fluxes of 409 ± 369 mmol m^{-2} d^{-1} for CO_2 and 1.6 ± 1.2 mmol m^{-2} d^{-1} for CH_4,

* Corresponding author at: 219 Ningliu Road, Nanjing 210000, Jiangsu Province, China.
E-mail address: zhhu@nuist.edu.cn (Z. Hu).

https://doi.org/10.1016/j.scitotenv.2020.144558

and made a disproportionately large, relative to the area, contribution to the total aquatic carbon emission of the watershed. Our results suggested the aquatic carbon emissions accounted for 6% of the watershed carbon budget, and fertilizer N and watersheds land use played a large role in the aquatic carbon emission.

1. Introduction

Carbon dioxide (CO_2) and methane (CH_4) are two crucial anthropogenic greenhouse gases contributing to global warming. As important conduits that link the land and oceans in global carbon transport, freshwaters (rivers, streams, lakes, and reservoirs) process large quantities of carbon and emit a disproportionately large amount of CO_2 (Raymond et al., 2013; Abril et al., 2014; Butman et al., 2016) and CH_4 (Bastviken et al., 2011; Borges et al., 2015; Stanley et al., 2016) to the atmosphere relative to their surface area. It is further estimated that the carbon gas emissions from freshwaters potentially offset a large portion of carbon uptake by land (Bastviken et al., 2011; Borges et al., 2015), suggesting the importance of inland waters in global carbon budget.

While several research efforts have been dedicated to quantify global freshwaters CO_2 and CH_4 emission fluxes, the current estimates are still poorly constrained. The estimated emission fluxes were 30–173 Tg C yr^{-1} for CH_4 (Bastviken et al., 2011; Kirschke et al., 2013) and 0.6–2.1 Pg C yr^{-1} for CO_2 (Cole et al., 2007; Aufdenkampe et al., 2011; Raymond et al., 2013), respectively, both showing considerable uncertainty. For fluvial networks alone, global estimates of CO_2 emission ranged from 0.2 Pg C yr^{-1} to 1.8 Pg C yr^{-1} with large uncertainty (Cole et al., 2007; Raymond et al., 2013; Lauerwald et al., 2015; Borges et al., 2015). The poorly constrained estimates were mainly due to the lack of widespread measurements and limited geographic distribution of the datasets for gas emission flux (Raymond et al., 2013; Borges et al., 2015). In particular, the gases emissions were associated with many complex watershed characteristics (e.g. wetland distribution, geomorphology, and human activity; Kortelainen et al., 2006; Huotari et al., 2013; Abril et al., 2014; Borges et al., 2018; Borges et al., 2019; Xiao et al., 2020). Field measurements across different land use types are needed to better understand the role of freshwaters in global carbon cycle.

Field studies showed that freshwater CO_2 and CH_4 concentrations were positively associated with the proportion of farmland area and agricultural practice intense in the watershed (Kortelainen et al., 2006; Borges et al., 2018). Intensive agriculture practices that use fertilizers can strongly impact regional carbon cycles within river networks, it will also enhance the availability of organic matter and nutrients to rivers, potentially stimulate the microbial processes and associated CO_2 and CH_4 productions (Bodmer et al., 2016; Borges et al., 2018; Wu et al., 2019). High CO_2 and CH_4 levels in farmland can contribute to the dissolved CO_2 and CH_4 concentrations in surrounding freshwater by surface drainage flows (Huotari et al., 2013; Wu et al., 2019). Agriculture occupies a large fraction of the global ice-free land surface area (Foley et al., 2005). Thus rivers impacted by agriculture across different regions deserve investigation to improve our ability in estimating the freshwaters CO_2 and CH_4 budget (Garnier et al., 2013; Huotari et al., 2013; Borges et al., 2015; Stanley et al., 2016).

China's Eastern plain has long been one of the most densely agricultural regions in the world. Intense agricultural practices have resulted in widespread pollution of surface water in this region (Qin et al., 2007; Yan et al., 2011). The total fertilizer N application rates in this region are about 470–600 kg N ha^{-1} yr^{-1} (Yan et al., 2011; Xiao et al., 2019a; Zhou et al., 2019), which was greatly higher than that in intensively agricultural regions in the US, France, and Sweden with a value less than 150 kg N ha^{-1} yr^{-1} (Garnier et al., 2013; Audet et al., 2017; Griffis et al., 2017). A significant fraction of agricultural N-fertilizer (~280 kg N ha^{-1} yr^{-1}) is lost to water body within the watershed by leaching and runoff (Yan et al., 2011; Xiao et al., 2019a; Zhou et al., 2019), which contributed eutrophication and have large impact on freshwater CO_2 and CH_4 emission (Beaulieu et al., 2019; Morales-Williams et al., 2020; Xiao et al., 2020). However, the riverine CO_2 and CH_4 emission in China's Eastern plain are poorly represented.

In this study, we investigated the rivers and lentic aquatic ecosystems (reservoir, ponds, and ditches) surface CO_2 and CH_4 dynamics in a typical subtropical agricultural-dominated watershed in Eastern China. Our main aims were to (1) investigate the spatiotemporal characteristics of CO_2 and CH_4 dynamics, (2) examine the factors that influence these variations, and (3) evaluate the importance of the freshwater in the watershed with intense agricultural practices, which can potentially act as sources of atmospheric CO_2 and CH_4 budgets. This study not only fills the gap in our knowledge of CO_2 and CH_4 dynamics in agricultural rivers, but also provides a valuable data source for aquatic carbon gas emission in such heavily agricultural regions. We hypothesized that the agricultural river acted as a significant CO_2 and CH_4 source given the significant fertilizer N application and further hypothesized that the aquatic carbon gas emission affected the watershed carbon balance.

2. Material and methods

2.1. Study area

The field sampling and measurements were carried out in an agricultural watershed, the Jurong Reservoir watershed (area 46 km^2) in Eastern China. The watershed (31°58′ to 32°01′N, 119°12′ to 119°14′E; elevation 30 m above sea level; Fig. 1) is located about 40 km southwest of Nanjing city, Jiangsu province. The watershed has been previously introduced in details (Yan et al., 2011; Li et al., 2013; Xia et al., 2013). In brief, regional land use is that rice paddies comprise 32.2% of the land use, cultivated upland comprises 22.8%, buildings and roads account for 27.5%, artificial forest and tea gardens cover 9.2%, and three rivers (River 1, west-river; River 2, middle-river; River 3, east-river; Fig. 1), a reservoir (Jurong Reservoir) and thousands of small ponds occupy the rest (8.3%). The area for the three rivers, the Jurong Reservoir, and ponds was 32 ha, 230 ha, and 110 ha, respectively. River width ranged from 2.6 m (upstream) to 4.4 m (downstream) in the longer rivers (River 1 and River 2), and it was approximately 3.4 m at the shortest river (River 3; Xia et al., 2013). Mean water depth in River 1, River 2, and River 3 were 0.6 m, 0.8 m, and 0.5 m, respectively. And the mean water depth for the reservoir and thousands of small ponds were 2.4 and 1.0 m, respectively. Previous studies showed the C/N of sediments were 8.38, 9.34, 8.07, 8.91, and 6.01 in River 1, River 2, River 3, pond, and reservoir (Li et al., 2013), respectively. The major cropping rotations are rapeseed-maize for the cultivated upland and wheat-rice for the paddy fields, respectively. There are no high livestock density and industry in the study region, and agricultural practices are the dominant local source of anthropogenic N discharging into the rivers, and underground pipe was not found. Sewage was another source of the N loading for rivers. High temperatures and rain occurred in the summer (from June to August), and low temperatures and rain occurred in the winter (from December to February in next year; Yan et al., 2011; Xiao et al., 2019a). The annual mean temperature and precipitation are about 15 °C and 1100 mm, respectively. With high fertilizer application (550–600 kg ha^{-1} yr^{-1}), a large amount of anthropogenic N was transported to the freshwaters of the watershed via runoff and leaching. Meanwhile, There was no external water source and the river discharge was dominated by precipitation and, it brings the

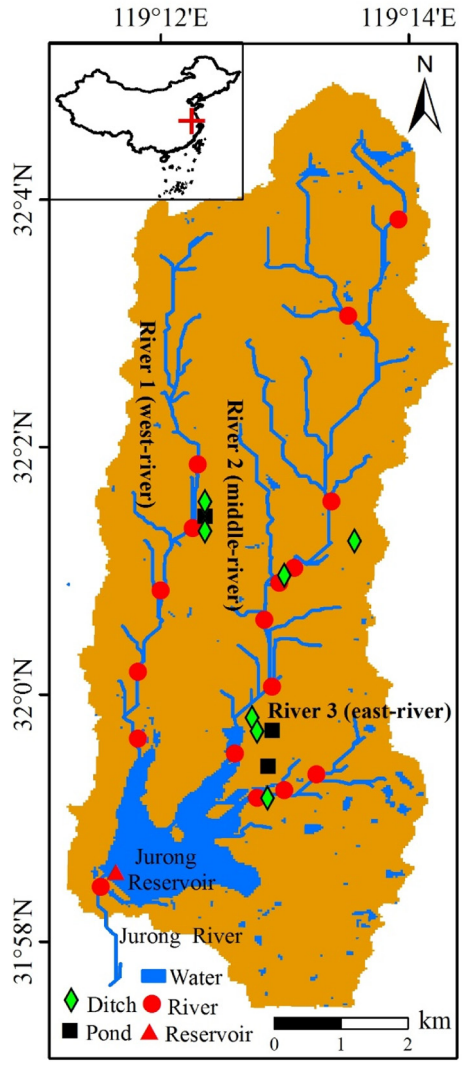

Fig. 1. Map showing the sampling sites in the agricultural-dominated watershed. The red dots denote sampling sites in rivers; black squares denote sampling sites in ponds; green diamonds denote sampling sites in ditches; red triangles denote sampling sites in reservoir. Water flows from the north to the south. The three rivers (River 1, River 2, and River 3) flow into the reservoir, and the water flows out via the Jurong River. The red cross in the illustration showing the location of the watershed in China. (For interpretation of the references to colour in this figure legend, the reader is referred to the web version of this article.)

three rivers with steady current velocity (greater than 0.01 m s^{-1} in rainy season) flowed into Jurong Reservoir. The only outlet of the watershed is the Jurong River located in the lowest part of the region (Fig. 1). In the watershed, the soil organic carbon contents ranged from 12 g kg^{-1} to 22 g kg^{-1} and total N from 0.75 g kg^{-1} to 1.22 g kg^{-1} (Yan et al., 2011).

2.2. Collection and analysis

Surface water was sampled from the three rivers (River 1, River 2, and River 3; Fig. 1) and ditches within the watershed to determine the dissolved CO_2 and CH_4 concentrations. From October 2015 to September 2017, watershed-scale sampling was carried out monthly, during which water was sampled at spatial sites across all water types (Fig. 1). In each watershed-scale survey, three surface (~20 cm) replicate bubble-free water samples were collected from each site. The total sampling site was 23, of which 5 sites in River 1, 8 sites in River 2, 3 sites in River 3 according to the river length, and 7 sites in ditches (Fig. 1). The sampling in River 1 contains two sections as the midstream and downstream, and in River 2 contains three sections with the upstream, midstream, and downstream. The sampling in ditches was non-continuous, because sometimes the ecosystem was dried up without available water. Water samples for dissolved CO_2 and CH_4 concentration measurements were also collected monthly in the lentic aquatic ecosystem (ponds and reservoir) and the outlet of the watershed (Jurong River) from October 2015 to September 2017 to estimate the aquatic ecosystem carbon emission of the watershed (Fig. 1).

Each field survey throughout the watershed was completed between 9:00 and 17:00 local time in two consecutive days. Triplicate bubble-free surface water was taken from the bridge or from the shore using organic glass hydrophore at each sampling site, and water samples for dissolved CO_2 and CH_4 measurements were transferred to 300 mL glass bottles via tubing. The glass bottle was immediately capped using a butyl stopper without headspace when excess water overflowing out, and the bottle was sealed with a sealing membrane after capping. Both of the hydrophore and glass bottles were washed with local water before sampling. Water samples were stored in ice-chilled coolers in the field, and were analyzed immediately when transported to laboratory within 48 h. The dissolved CO_2 and CH_4 concentrations in the samples were measured using headspace equilibration method. We had previously reported the procedures of sampling and analysis in details (Xiao et al., 2017; Xiao et al., 2019b). Specially, 100 mL water of the glass bottle was pushed out via injecting ultrahigh purity N_2 gas (99.999%) to create headspace. The glass bottle was then shaken vigorously about 5 min to allow the dissolved gases reach equilibrium between the residual liquid and the headspace. A small gas sample was drawn from the equilibrated headspace of the glass bottle via a syringe with three-way vale to determine the dissolved gas concentrations of water samples. The gas sample was injected into a gas chromatograph (Agilent GC7890B, Agilent, California, U.S.A.) fitted with flame ionization detector for CO_2 and CH_4 detection. The gas chromatograph was calibrated with standard gases (National Primary Standard prepared by the National Institute of Metrology, China) with mixing ratios of 352 ppm for CO_2 and 2 ppm for CH_4. Caution should be taken, because the mixing ratios of the standard gases were generally lower than that the partial pressure of CO_2 and CH_4 in the headspace. The dissolved CO_2 and CH_4 concentrations in the surface water were calculated according to measured CO_2 and CH_4 in equilibrated headspace and temperature-dependent Henry's law (Text S1 in Supporting Information).

In parallel to the CO_2 and CH_4 measurements, surface water samples were also collected to determine the dissolved inorganic nitrogen (nitrate (NO_3^--N), nitrite (NO_2^--N), and ammonium (NH_4^+-N)) concentrations. The dissolved inorganic nutrients concentrations (NO_3^--N, NO_2^--N, and NH_4^+-N) were measured via a flow injection analyzer (Skalar SAN+ +, The Netherlands) with high precision after filtration with Whatman GF/F filters (0.7-μm pore size). Concentrations of dissolved inorganic nutrients concentrations were analyzed within one week. The measurements of water temperature (T_w), dissolved oxygen concentration (DO), pH, specific conductance (Spc), and oxidation-reduction potential (ORP) were conducted in situ using a multi-parameter probe (YSI 650MDS, YSI Inc. Yellow Springs, OH, USA), which was calibrated before measurement. The measurements of DO showed a precision of ±0.1 mg L^{-1} and Spc showed a precision of ±0.001 mS cm^{-1}. Wind speed and precipitation were obtained from nearby weather station of the watershed during water sampling.

2.3. Saturation ratios and fluxes calculations

The saturation ratio for surface dissolved CO_2 and CH_4 was defined as:

$$\text{Saturation ratio} = C_w/C_{Eq} \quad (1)$$

where C_w is the surface dissolved gases (CO_2 and CH_4) concentrations (mmol m^{-3}) in water and measured by the headspace equilibration

method as described above. C_{eq} is the corresponding equilibrium gas concentration in water at in situ temperature, which was calculated based on atmospheric pressure, water temperature, and current atmospheric CO_2 (400 ppm) and CH_4 (2 ppm) mixing ratios (Xiao et al., 2017; Xiao et al., 2020). Saturation ratio can denote whether the water is a source (saturation ratio > 1; super-saturation) or sink (saturation ratio < 1; under-saturation) of the CO_2 and CH_4 to the atmosphere.

The fluxes of CO_2 and CH_4 across the water-air interface (F, unit in mmol m^{-2} d^{-1}, positive value denotes emission from the freshwater to the atmosphere) were estimated via the gas exchange model:

$$F = k \times (Cw - Ceq) \quad (2)$$

where k (m d^{-1}) was gas exchange velocity, and a common approach for k calculation was normalized to a Schmidt number of 600 (Cole and Caraco, 1998; Raymond et al., 2012):

$$k/k_{600} = (Sc/S_{c600})^{-n} \quad (3)$$

where S_c is the CO_2 and CH_4 Schmidt number at a given temperature, and the Schmidt number for CO_2 and CH_4 in these freshwaters were obtained from the study of Wanninkhof (1992); S_{c600} is the Schmidt number 600 corresponding to CO_2 and CH_4 at a temperature of 20 °C in freshwater; n is the Schmidt number exponent, and was assigned a value of 2/3 at low wind speed (<3.7 m s^{-1}) or 1/2 at high wind speed (>3.7 m s^{-1}). For rivers, k is controlled by channel physical factors such as velocity (v, m s^{-1}), depth (H, m), wind speed (U, m s^{-1}), and river slope (S, dimensionless; Raymond et al., 2012; Li et al., 2019). For River 1, River 2, River 3, and Jurong River in this study, the k_{600} (m d^{-1}) was calculated according to the study of Raymond et al. (2012):

$$k_{600} = (v \times S) \times 2841 + 2.02 \quad (4)$$

Although Raymond et al. (2012) found the k in rivers was the product of velocity and slope, several formulations consider both velocity and wind speed (e.g. Clough et al., 2007) for k calculation. For comparison, the study also estimated the k considering both velocity and wind speed (Text S2).

For the reservoir, pond and ditch, the k calculation was dependent on wind speed in these lentic ecosystems. The k (m d^{-1}) was calculated according to Cole and Caraco (1998):

$$k = 0.24 \times ((S_c/600)^{-n} \left(2.07 + 0.215 \times U^{1.7}\right) \quad (5)$$

where 0.24 was used for the conversion of cm h^{-1} to m d^{-1}.

2.4. Data analysis

Simple linear and multi-linear regressions were carried out to find relationships between CO_2 dynamics, CH_4 dynamics, and environmental variables. For each field survey, the mean dissolved gases (CO_2 and CH_4) concentrations were computed using all measurements within the corresponding water type for analysis of temporal variability, the ditches were excluded due to non-continuous sampling. Measurements made at each of all sampling sites in rivers were averaged over the two-year measurement period for analysis of spatial variability. The differences of mean gases concentrations across seasons (spring, from March to May; summer, from June to August; autumn, from September to November; and winter, from December to February in next year) and water types were determined using a least significant difference by SPSS (version 18.0). Differences at the level of $p < 0.05$ were considered statistically significant, and normality of data was tested. Moreover, Monte Carlo simulations were performed to assess uncertainties in extrapolating monthly sampling to the annual flux estimations for each water body. The Monte Carlo procedure assumed a normal distribution and randomly picked values from the C-gases flux, and the standard deviation of the annual mean C-gases fluxes was based on a total of 10,000 Monte Carlo ensemble members. River morphology was considered in the calculation of total C-gases evasion from the three sampling rivers due to the large difference in river length.

3. Results

3.1. Environmental variables

Water temperature in the different freshwaters of the watershed is remarkably uniform, and the temperature variation was <0.6 °C between water types (Table 1). The annual mean water temperature was 19.1 ± 8.5 °C, showing seasonality: summer (29.3 ± 2.7 °C) > spring (19.4 ± 4.8 °C) > autumn (18.9 ± 6.3 °C) > winter (8.7 ± 2.7 °C; Fig. S1). Precipitation occurred in each month with peak in summer (Fig. S1).

In contrast to water temperature, the dissolved inorganic nitrogen concentrations varied. On average, the highest NO_3^--N concentration with a mean value of 1.85 ± 1.81 mg L^{-1} occurred in ditches and lowest in ponds with a mean value of 0.45 ± 0.45 mg L^{-1}. However, peak NH_4^+-N concentration occurred in ponds (0.32 ± 0.36 mg L^{-1}) and the lowest in ditches (0.12 ± 0.15 mg L^{-1}). The highest DO occurred in the reservoir and the lowest in ponds (Table 1). Generally, the NO_3^--N concentration was higher than the NH_4^+-N concentration, and accounted for 57% ~ 92% of the total dissolved inorganic concentration in the aquatic ecosystems. For the three major rivers (River 1, River 2, and River 3), the temporal variation of NO_3^--N concentration were highly intercorrelated, for example, the concentration in River 1 was highly correlated with that in River 3 ($r = 0.84$, $p < 0.01$). It should be noted that these variables showed insignificant ($p > 0.05$) differences between the three rivers, but significant ($p < 0.05$) differences were found among different water types.

3.2. Surface CO_2 and CH_4 concentrations

The CO_2 and CH_4 concentrations varied across water types (Fig. 2). The mean concentrations of CO_2 and CH_4 in River 3 were significantly higher ($p < 0.01$) than that in River 1, River 2, pond, reservoir, and the outlet of the watershed, Jurong River (Table S1). The ditches also had high CO_2 and CH_4 concentrations with mean values of 107 ± 66 μmol L^{-1} and 963 ± 1959 nmol L^{-1}, respectively. The lowest concentrations occurred in the reservoir with mean values of 28 ± 17 μmol L^{-1} for CO_2 and 116 ± 77 nmol L^{-1} for CH_4. Based on the measurement of River 1, River 2, and River 3, the average CO_2 and CH_4 concentrations in the river network were 112 ± 36 μmol L^{-1} and 509 ± 341 nmol L^{-1}, respectively.

The CO_2 concentration in the three major rivers varied seasonally, with peak values generally appearing in the summer (Fig. 3a). The mean CO_2 concentrations in the summer with values of 155 ± 69 μmol L^{-1} (River 1), 162 ± 51 μmol L^{-1} (River 2), and 243 ± 72 μmol L^{-1} (River 3) were significantly ($p < 0.01$) higher than those in the winter with corresponding mean values of 44 ± 41 μmol L^{-1}, 55 ± 46 μmol L^{-1}, and 68 ± 69 μmol L^{-1}, however, the differences between spring and winter were insignificant ($p > 0.05$). For the other freshwater types (ponds, reservoir, and Jurong River), the monthly CO_2 concentrations varied within a relatively narrow range (Fig. 3a), showing insignificant ($p > 0.05$) differences between seasons.

The monthly CH_4 concentration varied temporally (Fig. 3b). On average, the highest CH_4 concentration generally occurred in the summer except for River 1, in which the highest concentration occurred in spring and winter. It should be noted that the average summertime CH_4 concentration with a mean value of 204 ± 55 nmol L^{-1} was significantly ($p < 0.01$) higher than that in spring, autumn, and winter in the lentic reservoir, but the differences among seasons were insignificant ($p > 0.05$) in River 2, ponds, and Jurong River.

Table 1
Summary of the annual mean surface water temperature (T_w), dissolved inorganic concentration (NH_4^+-N, NO_3^--N, and NO_2^--N), and DO concentration in all water types during measurement period from October 2015 to September 2017. The presented values are the mean ± standard deviation.

Sample type	Water temperature (°C)	NH_4^+-N (mg L^{-1})	NO_3^--N (mg L^{-1})	NO_2^--N (mg L^{-1})	DO (mg L^{-1})
River 1	19.4 ± 8.5	0.30 ± 0.25	1.02 ± 0.56	0.05 ± 0.04[a]	7.16 ± 4.36
River 2	19.2 ± 8.5	0.23 ± 0.15	0.92 ± 0.68	0.05 ± 0.07	7.10 ± 4.13
River 3	19.2 ± 8.5	0.26 ± 0.17	1.08 ± 0.67	0.04 ± 0.04	6.30 ± 3.95
Ponds	19.2 ± 8.4	0.32 ± 0.36	0.45 ± 0.45	0.03 ± 0.05	5.78 ± 4.09
Reservoir	19.6 ± 8.5	0.17 ± 0.10	0.56 ± 0.34	0.02 ± 0.02	9.59 ± 3.38
Jurong River	19.0 ± 8.5	0.16 ± 0.10	0.51 ± 0.32	0.03 ± 0.02	8.36 ± 5.10
Ditches	18.3 ± 5.9	0.12 ± 0.15	1.85 ± 1.81	0.04 ± 0.04	7.90 ± 2.04

River 3 with short length had the highest CO_2 and CH_4 concentrations compared to River 1 and River 2. Large spatial variability for the surface CO_2 and CH_4 concentration in River 2 was found (Fig. 4). The average concentrations of CO_2 (128 ± 47 μmol L^{-1}) and CH_4 (572 ± 748 nmol L^{-1}) in upstream of River 2 were significantly ($p < 0.01$) higher than those in midstream (CO_2: 87 ± 60 μmol L^{-1}; CH_4: 300 ± 236 nmol L^{-1}) and downstream (CO_2: 72 ± 59 μmol L^{-1}; CH_4: 323 ± 201 nmol L^{-1}).

3.3. Correlations between CO_2, CH_4 saturation ratios and environmental variables

Our data showed that dissolved CO_2 and CH_4 were supersaturated with respect to the atmosphere in most of the sampled sites, suggesting this agricultural-dominated freshwaters were almost net sources of atmospheric CO_2 and CH_4. The mean CO_2 saturation ratio were 6.0 ± 4.3 in River 1, 5.8 ± 4.5 in River 2, 9.3 ± 6.8 in River 3, 1.6 ± 1.2 in the reservoir, 5.8 ± 5.2 in ponds, 6.1 ± 3.8 in ditches, and 2.7 ± 3.1 in Jurong River. The corresponding CH_4 saturation ratios were 88 ± 61, 119 ± 74, 256 ± 273, 40 ± 32, 126 ± 169, 300 ± 576, and 41 ± 61. Based on the measurement of River 1, River 2, and River 3, the average CO_2 and CH_4 saturation ratios in the river network were 7.1 ± 1.9 and 154 ± 90, respectively. To better understand the potential controls of CO_2 and CH_4 saturations, we analyzed the correlations between the saturations and each of the main environmental variables.

Results showed the temporal variation of CO_2 and CH_4 saturations depended on some environmental variables (Table 2). The monthly CO_2 saturations in all freshwaters were positively correlated with water temperature (Table 2). Temporal CO_2 saturation was positively related to NO_2^--N in River 1, River 2, and reservoir, with NH_4^+-N in River 2 and Jurong River, and with precipitation in River 1. The CO_2 saturation was negatively related with DO in River 3 and ponds, and with ORP in River 1, River 2, and River 3. The temporal CH_4 saturation was positively related with water temperature except in River 1, and negatively related to ORP except in River 1 and River 2. The nutrient concentrations were positively related with temporal CH_4 saturation in River 3 and reservoir. It is important to note that the temporal CH_4 saturations were positively correlated with precipitation in River 3 and ponds (Table 2). Multi-linear stepwise regression analysis revealed that water temperature and NH_4^+-N together explain 72% ($R^2 = 0.72$, $p < 0.01$) of observed temporal variability of CO_2 saturation in River 2.

Significant correlations between spatial variations of the gas saturations and some of the explanatory variables were found in river network (Figs. 5 and 6). The spatial CO_2 and CH_4 saturations were both positively correlated with the concentrations of NO_3^--N and NO_2^--N (Fig. 5), and negatively correlated with DO concentration (Fig. 6). It should be noted that spatial variation in DO concentration explained 64% and 66% of the observed variance in CO_2 ($R^2 = 0.64$, $p < 0.01$; Fig. 6a) and CH_4 ($R^2 = 0.66$, $p < 0.01$; Fig. 6b), respectively. Importantly, spatial CO_2 saturation was highly correlated with that CH_4 saturation in river network ($R^2 = 0.90$, $p < 0.01$; Fig. 6c).

3.4. Surface CO_2 and CH_4 fluxes

The aquatic diffusion CO_2 and CH_4 fluxes of the agricultural watershed were estimated using the water-air gas exchange model above.

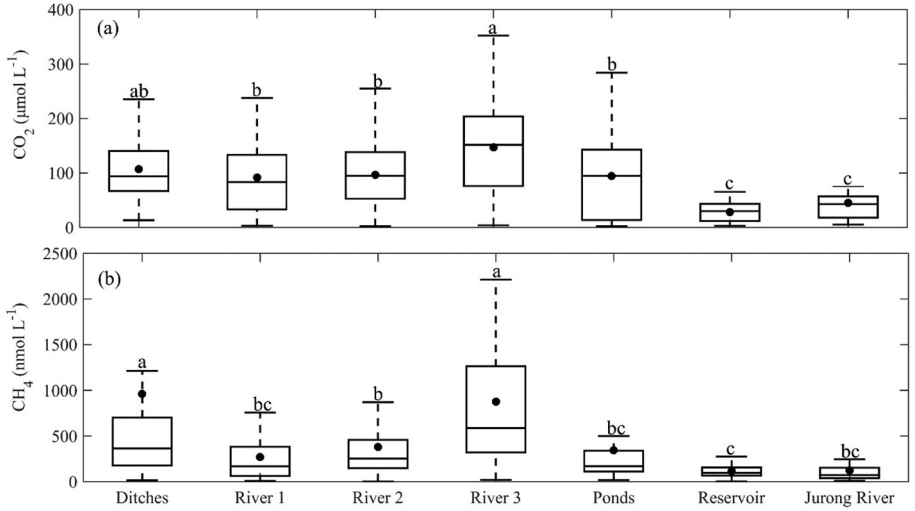

Fig. 2. Surface dissolved CO_2 concentration (a) and CH_4 concentration (b) for ditch, rivers (River 1, River 2, River 3, and Jurong River), pond, and the reservoir. Boxes are bounded by the 25th and 75th percentiles and show the median (solid lines), horizontal lines indicate the 10th and 90th percentiles, black circles are outliers, black dots show the mean values (the same below). Different letters indicate significant differences at $p < 0.05$ across water types.

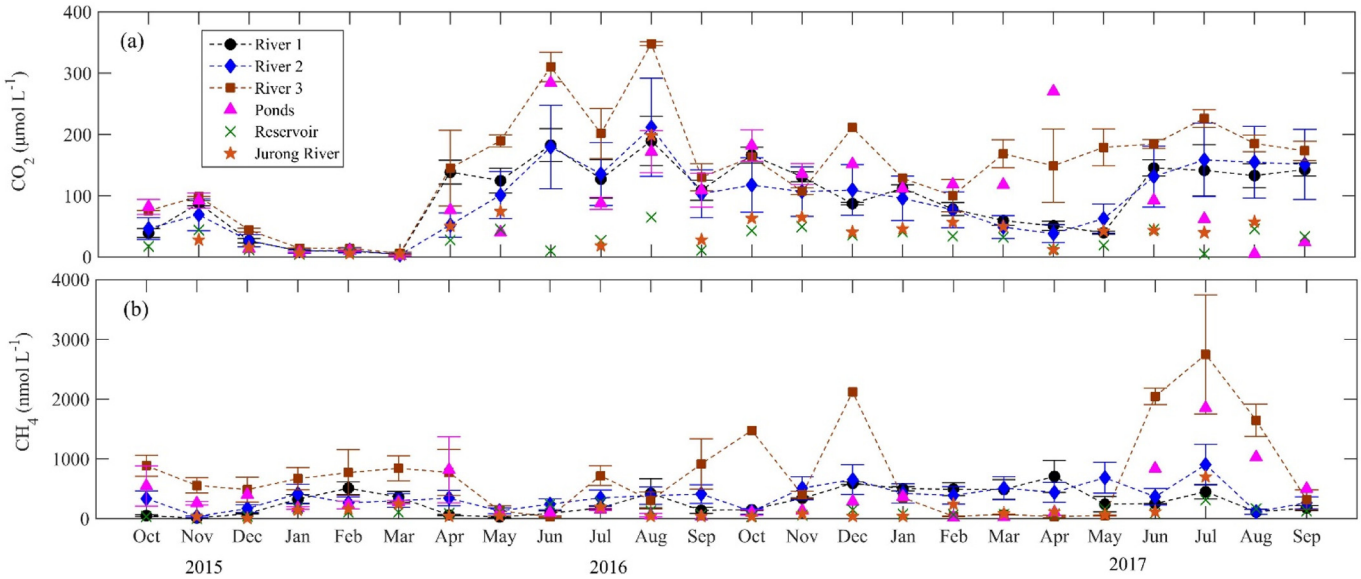

Fig. 3. Monthly variations of CO_2 concentration (a) and CH_4 concentration (b) for rivers (River 1, River 2, River 3, and Jurong River), ponds, and the reservoir from October 2015 to September 2017. Error bars represent standard error.

The mean gas exchange velocity for flux calculation was 4.87 m d^{-1} for CO_2 and 4.80 m d^{-1} for CH_4 in rivers, and was 0.84 m d^{-1} for CO_2 and 0.82 m d^{-1} for CH_4 in lentic aquatic ecosystems. The estimated surface aquatic CO_2 flux across site and time ranged from −70 mmol m^{-2} d^{-1} to 2070 mmol m^{-2} d^{-1}, with an annual mean value of 272 ± 262 mmol m^{-2} d^{-1}, suggesting the water was significant sources of atmospheric CO_2. The highest CO_2 flux occurred in River 3 with an annual mean value of 690 ± 558 mmol m^{-2} d^{-1} and the lowest in the reservoir with an annual mean value of 13 ± 24 mmol m^{-2} d^{-1}. The average diffusion CO_2 fluxes from River 1, River 2, ponds, and ditches were 377 ± 333 mmol m^{-2} d^{-1}, 403 ± 379 mmol m^{-2} d^{-1}, 70 ± 82 mmol m^{-2} d^{-1}, and 84 ± 46 mmol m^{-2} d^{-1}, respectively. Based on the measurement of River 1, River 2, and River 3, the average CO_2 evasion from the three sampling rivers was estimated as the area-weighted mean of the each river flux considering the shortest River 3 had the highest emission flux. The area-weighted mean CO_2 emission flux from the river network was 409 ± 369 mmol m^{-2} d^{-1}.

Similar to CO_2, the aquatic diffusion CH_4 flux ranged from less than 0.1 mmol m^{-2} d^{-1} to 16.5 mmol m^{-2} d^{-1}, with an annual mean value of 1.3 ± 1.2 mmol m^{-2} d^{-1}, suggesting the water was constant source of atmospheric CH_4. River 3 had the highest diffusion CH_4 flux, with a mean value of 3.7 ± 4.1 mmol m^{-2} d^{-1}, followed by River 2 (1.8 ± 1.2 mmol m^{-2} d^{-1}), River 1 (1.2 ± 0.8 mmol m^{-2} d^{-1}), and ditches (0.6 ± 1.1 mmol m^{-2} d^{-1}). The lowest aquatic diffusion CH_4 flux occurred in the reservoir with a mean value of 0.1 ± 0.1 mmol m^{-2} d^{-1}. The annual mean diffusion CH_4 flux from ponds was 0.4 ± 0.4 mmol m^{-2} d^{-1}. Similar to CO_2, the estimated CH_4 emission flux from the river network was 1.6 ± 1.2 mmol m^{-2} d^{-1}.

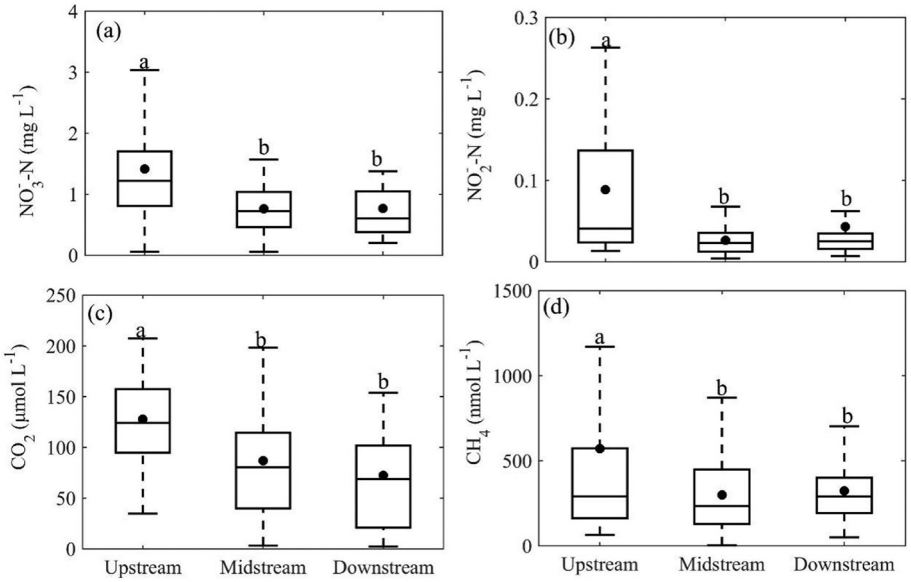

Fig. 4. The spatial gradient of NO_3^--N concentration (a), NO_2^--N concentration (b), CO_2 concentrations (c), and CH_4 concentration (d) in River 2. Headwaters were defined as upstream, the locations near the reservoir were defined as downstream, and others were defined as midstream. The number of sampling sites in upstream, midstream, and downstream in River 2 were 3, 3, and 2, respectively. Different letters indicate significant differences at $p < 0.05$.

Table 2
Correlations between monthly CO_2 saturation ratio, CH_4 saturation ratio and environment variables from October 2015 to September 2017 across different water types[a].

Sample type	Gases	T_w	NH_4^+-N	NO_3^--N	NO_2^--N	DO	ORP	P[d]
River 1	CO_2	0.77[b]	−0.15	−0.23	0.43[c]	−0.32	−0.56[b]	0.38[c]
	CH_4	−0.03	−0.05	0.13	0.05	−0.33	0.21	−0.01
River 2	CO_2	0.80[b]	0.58[b]	0.19	0.53[c]	−0.19	−0.50[c]	0.31
	CH_4	0.35[c]	0.23	0.01	0.14	−0.28	−0.36	0.15
River 3	CO_2	0.82[b]	0.02	−0.60[b]	0.19	−0.58[b]	−0.45[c]	0.22
	CH_4	0.36[c]	−0.01	0.10	0.46[c]	−0.23	−0.50[c]	0.65[b]
Ponds	CO_2	0.39[c]	0.05	−0.11	0.05	−0.49[c]	−0.28	0.11
	CH_4	0.42[b]	−0.19	−0.23	−0.21	−0.25	−0.50[c]	0.48[c]
Reservoir	CO_2	0.43[c]	0.20	0.01	0.43[c]	−0.29	−0.10	0.27
	CH_4	0.67[b]	0.60[b]	0.12	0.19	0.08	−0.46[c]	0.14
Jurong River	CO_2	0.47[c]	0.55[c]	−0.21	0.23	−0.41	−0.13	−0.01
	CH_4	0.40[c]	−0.13	−0.26	−0.19	0.01	−0.58[c]	0.23

[a] The total number of observations is 24, resenting monthly samplings from October 2015 to September 2017.
[b] Correlation is significant at the 0.01 level.
[c] Correlation is significant at the 0.05 level.
[d] Precipitation, the 10-day accumulated precipitation (mm) before each sampling.

4. Discussion

4.1. Impact of fertilizer N application

The freshwaters of the watershed can be characterized as heavily polluted area due to high agriculture cover with significant fertilizer N application (Qin et al., 2007; Yan et al., 2011; Xiao et al., 2019b). The observed nutrient concentrations (e.g. NO_3^--N; Table 1) in the river were similar to or higher than those in other agricultural rivers with NO_3^--N concentration ranging concentration from 0.18 mg L^{-1} to 1.81 mg L^{-1} (Bodmer et al., 2016; Borges et al., 2018; Zhang et al., 2020). The surface water was supersaturated with dissolved CO_2 and CH_4 concentrations, and the gas saturation ratios in river network were positively correlated with nutrient concentrations (Fig. 5), suggesting the input of fertilizer N can largely affect the aquatic CO_2 and CH_4 production and emission (Bodmer et al., 2016; Ollivier et al., 2019; Xiao et al., 2020). Specifically, the mean NO_3^--N and NO_2^--N concentrations in upstream were significantly higher than that in midstream and downstream within River 2 (Figs. 4a-4b), corresponding to the significantly ($p < 0.01$) higher CO_2 and CH_4 concentrations in upstream (Figs. 4c-4d). However, it should

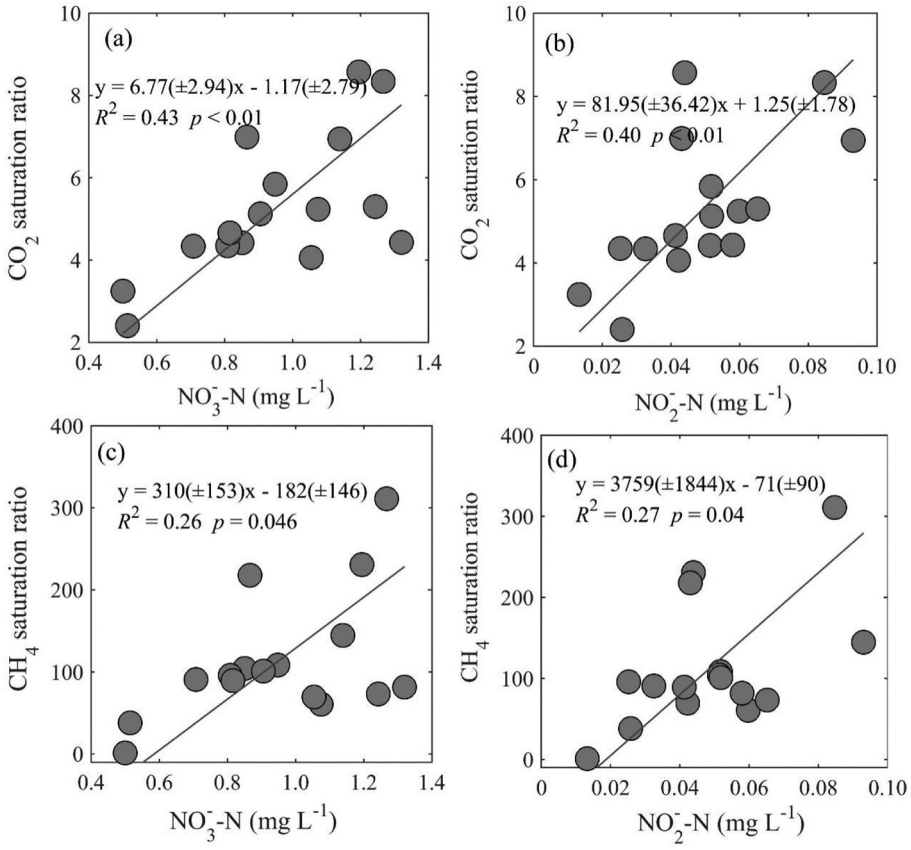

Fig. 5. Spatial correlations between mean CO_2 saturation ratio and NO_3^--N concentration (a), between mean CO_2 saturation ratio and NO_2^--N concentration (b), between mean CH_4 saturation ratio and NO_3^--N concentration (c), and between mean CH_4 saturation ratio and NO_2^--N concentration (d). Each data point represents the mean value at one spatial sampling site in river network from October 2015 to September 2017. Parameter bounds on the regression coefficients indicate 95% confidence limits.

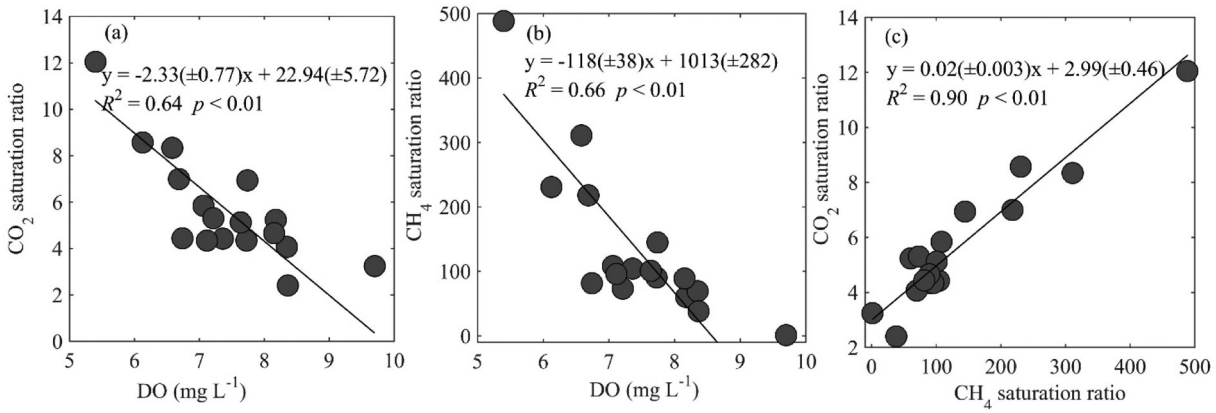

Fig. 6. Spatial correlations between mean CO_2 saturation ration and DO concentration (a), between mean CH_4 saturation ratio and DO concentration (b), and between mean CO_2 saturation ratio and CH_4 saturation ratio (c) in river network during measurement period. Each data point represents the mean value at one spatial sampling site in river network from October 2015 to September 2017. Parameter bounds on the regression coefficients indicate 95% confidence limits.

be noted that direct CO_2 and CH_4 input from other sources (e.g. soil and groundwater) could increase the dissolved CO_2 and CH_4 (Richey et al., 2002; Humborg et al., 2010; Striegl et al., 2012; Duvert et al., 2018), and the input of CO_2 and CH_4 may be accompanied by high N loadings (Xiao et al., 2017; Xiao et al., 2020). Our results reported here suggest the fertilizer N loadings can be a good indicator of watershed changes on CO_2 and CH_4 variability within river.

The large differences in the CO_2 and CH_4 concentrations between and within the water bodies support the role of watershed land use and associated fertilizer N input. The aquatic CO_2 and CH_4 concentrations varied across water types with the highest CO_2 concentration occurred in rivers and the highest CH_4 concentration in ditches (Fig. 2), which were also associated with the nutrient availability. For example, the average NO_3^--N concentration in rivers (1.01 mg L^{-1}) and ditches (1.85 mg L^{-1}) were significantly ($p < 0.01$) higher than that in other aquatic ecosystems (Table 1) due to the watershed land use as shown in previous studies (Xia et al., 2013). For comparison among different rivers, the shortest River 3 had the highest concentrations of CO_2 (147 μmol L^{-1}) and CH_4 (877 nmol L^{-1}) compared to River 1 and River 2 (Fig. 2). River 3 had the highest population density with intensive anthropogenic disturbance (Xia et al., 2013), potentially suggesting the role of watershed land use in CO_2 and CH_4 variability. Previous study also found that watershed land use change (e.g. agriculture land cover) could affect dissolved inorganic nitrogen and associated greenhouse gas concentration in rivers (Borges et al., 2018). Additionally, CO_2 production in streams and rivers is closely related not only to the internal carbon dynamics, but also to the biogeochemical processes of terrestrial ecosystem within the watershed, including the influx of soil CO_2 and wetland CO_2 and in situ aqueous respiration of organic carbon (Striegl et al., 2012; Duvert et al., 2018; Borges et al., 2019; Xiao et al., 2020). Our results are consistent with previous studies showing watershed land use change could affect the freshwater CO_2 and CH_4 variations (Stanley et al., 2016; Borges et al., 2018; Smith et al., 2017).

Another notable feature was that DO could well explain the spatial variability of CO_2 and CH_4 in river network. Our results found the CO_2 and CH_4 saturations were negatively correlated with DO concentration (Fig. 6), which were consistent with previous studies (Kortelainen et al., 2006; Campeau and Del Giorgio, 2014; Xiao et al., 2017; Borges et al., 2018; Xiao et al., 2020). The high N loadings will contribute to the CO_2 and CH_4 production via stimulating microbial activities and increasing oxygen consumption (Bodmer et al., 2016; Wang et al., 2017; Hu et al., 2018; Ollivier et al., 2019). High nutrient loadings-induced oxygen consumption can also suppress the CH_4 oxidation and maintain high dissolved CH_4 concentration (Xiao et al., 2017). A positive relationship between CO_2 saturation and CH_4 saturation (Fig. 6c) suggested a level of common regulation for the two gases (Campeau and Del Giorgio, 2014; Borges et al., 2018). Considering DO was associated with watershed land us (e.g. agriculture cover) and external N input (Borges et al., 2018; Xiao et al., 2019a). In this regard, the DO effects may indicate the role of land use change in the agricultural-dominated watershed. Meanwhile, the relationship between CO_2 and DO can explain the role of respiration and photosynthesis process in aquatic systems. Our results reported here are consistent with the field measurement in urban rivers (Yu et al., 2017; Hu et al., 2018), showing DO was a useful parameter in explaining CO_2 and CH_4 dynamic variability.

4.2. Factors influencing the CO_2 and CH_4 temporal variation

The temporal variations of CO_2 saturation significantly increased with water temperature in all water bodies of the watershed (Table 2). Temperature played a large role in determining CO_2 production and emission, for example, temperature explained 67% ($R^2 = 0.67$, $p < 0.01$) of the observed temporal variability in the CO_2 saturation in River 3. Our results suggested that high water temperature may stimulate the in situ CO_2 production rate and promote dissolved CO_2 saturation (Striegl et al., 2012; Wang et al., 2017; Borges et al., 2018; Yang et al., 2018). It should be noted that the role of temperature varied among water bodies (Table 2). The notable feature was that more significant correlation in river network with high nutrient loadings, suggesting the effect of temperature may be amplified with external N loadings.

Previous study demonstrated that temperature played a key role in aquatic CH_4 temporal variation (Yvon-Durocher et al., 2014). The aquatic CH_4 level increased significantly with increasing temperature (Campeau and Del Giorgio, 2014; Xiao et al., 2017; Yang et al., 2018; Borges et al., 2018). In this study, high CH_4 concentrations generally occurred in warm seasons, and the correlations between temperature and monthly CH_4 saturation were significant except for River 1 (Table 2). However, some peak CH_4 concentrations occurred in winter (Fig. 3b), this may be explained by high dissolved organic carbon concentration at that time with a value of 18.6 mg L^{-1}, compared to the value of 6.3 mg L^{-1} in the summer (Zhao et al., 2013), because high dissolved organic carbon would increase substrate availability and stimulate CH_4 production (Crawford and Stanley, 2016; Ma et al., 2018; Yang et al., 2019). Meanwhile, a more significant correlation was found in reservoir with relatively low nutrient loadings. These suggested that the other factors, such as nutrient loadings and dissolved organic concentration, also regulated the CH_4 temporal variation (Schrier-Uijl et al., 2011; Ma et al., 2018; Wu et al., 2019; Yang et al., 2019).

Temporal vacations in CO_2 and CH_4 saturations were associated with precipitation and nutrient concentrations (Table 2). Monthly CH_4 saturation was positively correlated with precipitation in small ponds and River 3 with high nutrient loadings (Table 2). Precipitation could transport more agricultural nutrient and carbon loadings to the aquatic ecosystems (Dinsmore et al., 2013; Sinha et al., 2017), and then increase dissolved CH_4 saturation via stimulating production rate (Stanley et al., 2016; Yu et al., 2017). Heavy precipitation of the watershed often occurred in the rice-growing period (Yan et al., 2011), which could deliver more CH_4-rich water from rice paddies to river and pond (Wu et al., 2019). Additionally, the temporal CO_2 saturation in River 1 was positively correlated with precipitation (Table 2), frequent precipitation and high temperature in the summer of the watershed would enhance production and lateral transport of soil CO_2, probably contributing to the high CO_2 in rivers (Richey et al., 2002; Humborg et al., 2010). Temporal variations of the C-gases saturations were positively correlated with nutrient concentrations, except in River 3. The nutrient concentrations varied temporally, which were associated with agricultural activities (Xia et al., 2013; Xiao et al., 2019a). These may suggest that agricultural activities could influence the temporal pattern of C-gases dynamics.

Precipitation-induced river discharge in this study (Yan et al., 2011; Xia et al., 2013) may influence the gas temporal variation. Freshwater discharge is known to be a major driver of the seasonal variability of CO_2 and CH_4 (Borges et al., 2018). Heavy precipitation in summer (Fig. S1) increased the river discharge and then may confound the temperature influence. These may be an alternative explanation for the poor correlation between CH_4 and temperature in river (e.g. River 1; Table 2) and some peak CH_4 concentration occurring in winter with low river discharge, which also had been found in other studies (Xiao et al., 2017; Borges et al., 2018).

4.3. Comparison of the CO_2 and CH_4 fluxes with other published studies

In this study, we found the aquatic CO_2 and CH_4 were oversaturated and acted as sources of atmospheric CO_2 and CH_4. The CO_2 emission flux with an annual mean value of 409 mmol m^{-2} d^{-1} in river network was compared with those in urban rivers with high pollutant loadings in China (Wang et al., 2017; Yu et al., 2017; Hu et al., 2018), and was higher than that in the Amazon basin with a mean value of 190 mmol m^{-2} d^{-1} (Richey et al., 2002). Our results showed that the rivers were significant sources of atmospheric CO_2 compared to other studies worldwide (Table 3). The CO_2 emission flux from the reservoir (13 mmol m^{-2} d^{-1}) was lower than from China's reservoirs with a mean value of 44 mmol m^{-2} d^{-1} (Li et al., 2018). However, the emission flux from ponds with a mean value of 70 mmol m^{-2} d^{-1} was higher than from China's lakes and ponds (Li et al., 2018), suggesting small ponds with high nutrient loadings played an essential role in inland water CO_2 budget (Holgerson and Raymond, 2016). Additionally, large amount of fertilizer N discharged into ditches (Table 1; Xiao et al., 2019a), likely leading to the ecosystem was hotspot of CO_2 with a mean emission flux of 84 mmol m^{-2} d^{-1}. This is consistent with the study of Ollivier et al. (2019) which showed small agricultural water can be a major source of CO_2 emission.

The mean diffusion CH_4 flux from the river network was 1.6 mmol m^{-2} d^{-1}. As shown in Table 3, the river network was also significant source of atmospheric CH_4. The diffused CH_4 flux in ponds (0.4 mmol m^{-2} d^{-1}) was higher than the global average for lakes and ponds with a value of 0.1 mmol m^{-2} d^{-1} (Holgerson and Raymond, 2016). For comparison, the diffusion flux from a eutrophic lake nearby was 0.1 mmol m^{-2} d^{-1} (Xiao et al., 2017). The low diffusion of CH_4 flux in the reservoir (0.1 mmol m^{-2} d^{-1}) in this study may result from the low nutrient loadings and high DO concentration compared to the global reservoirs (Deemer et al., 2016). Meanwhile, high nutrient concentrations and relative low DO concentration probably led to the high diffusion CH_4 flux (0.6 mmol m^{-2} d^{-1}) in ditches.

When taking into account the surface area of each water type (Yan et al., 2011; Xia et al., 2013), the aquatic carbon emission was 1.12 Gg C yr^{-1} for CO_2 and 0.006 Gg C yr^{-1} for CH_4, respectively. The river network only occupied 8% of total surface water area, but accounted for 51% of total aquatic carbon emission due to significantly higher CO_2 and CH_4 emission rates. The ponds with the highest NH_4^+-N concentration (Table 1) accounted for considerable fraction (29%) of the total aquatic carbon emission, and reservoir and ditches accounted for 12% and 8% of total aquatic carbon emission, respectively. Based on the net primary productivity measurements in the basin (Xu et al., 2017), we estimated that about 6% of net primary production of the watershed was lost as aquatic carbon emission. The fraction was higher than that in the English Lake District and Lake Taihu basin with values less than 2% (Maberly et al., 2013; Xiao et al., 2020), but fall in low range in the existing literature with value reaching to 27% (Butman et al., 2016; Yu et al., 2017). Our results suggest that the net primary productivity of the watershed (defined as terrestrial only) would be overestimated by 6%, and aquatic carbon flux is necessary to accurately estimate the watershed carbon budget (Butman et al., 2016).

The estimation of CO_2 and CH_4 exchange fluxes across water-air interface needs an a priori delineation of regions where actual value of gas exchange velocity k was reported. Like other studies (Raymond et al., 2013; Lauerwald et al., 2015), the estimation of k in this study was associated with uncertainties in CO_2 and CH_4 fluxes estimation. Different equations for k calculation have been proposed, and our study also found the k values varied between two equations (Eq. (4) versus Eq. (S2)). The ultimate flux was estimated via Eq. (4) in this study, because the equation was scaled from 563 direct measurements covering a wide range of environmental conditions (Raymond et al., 2012). However, the channel slope was not measured, and was obtained from other

Table 3
Comparison of the CO_2 and CH_4 dynamics in rivers across different countries and climate zones.

Regional/Country	CO_2		CH_4		Reference
	Concentration	Flux	Concentration	Flux	
Jurong watershed in Eastern China	112 ± 36	409 ± 369	509 ± 341	1.6 ± 1.2	This study
Urban rivers in Tianjin, China	38	20	1350	1.7	Hu et al. (2018)
Urban rivers in Shanghai, China	234	243–1078	390	0.3–24.7	Yu et al. (2017)
Urban rivers in Chongqing, China	80	447			Wang et al. (2017)
Rivers in Africa	186	186–1149	2205	0.5–18	Borges et al. (2015)
Rivers in USA		541			Butman and Raymond (2011)
Rivers in Sweden		422			Humborg et al., 2010
Rivers in Amazon basin		190–465			Lauerwald et al. (2015)
Rivers in northern Germany	110		792		Bodmer et al. (2016)
46 rivers in boreal zone	130	81	1225	1.1	Campeau and Del Giorgio (2014)
Rivers in southern Finland		386		5.9	Huotari et al. (2013)
Yukong River in USA	>68	87	15	0.6	Striegl et al. (2012)

The units for concentration are μmol L^{-1} for CO_2 and nmol L^{-1} for CH_4, respectively, and the unit for flux is mmol m^{-2} d^{-1}.

studies according to the river characterization (Lauerwald et al., 2015; Fu et al., 2018). These may lead to the uncertainty in the *k* estimation, which was associated to considerable uncertainties in CO_2 and CH_4 fluxes. Considering the dissolved concentrations controlled the gas emission across the water-air interface (Holgerson and Raymond, 2016; Xiao et al., 2017; Xiao et al., 2020), the large CO_2 and CH_4 concentrations reported here also suggested the freshwaters were significant atmospheric CO_2 and CH_4 sources.

5. Conclusion

Two-year (2015–2017) field measurements showed that the surface CO_2 and CH_4 dynamics varied across different water types. Peak CO_2 and CH_4 concentrations occurred in the aquatic ecosystem with higher nutrient concentration, suggesting the role of watershed land use and fertilizer N loadings. The mean CO_2 and CH_4 saturation ratios were oversaturated, indicating these aquatic ecosystems were sources of atmospheric CO_2 and CH_4.

In river network, dissolved inorganic nitrogen concentration and dissolved oxygen concentration were correlated with the observed spatial variability in CO_2 and CH_4 saturation rations. Additionally, temporal variations in surface aquatic CO_2 and CH_4 saturation ratios were positively correlated with water temperature.

About 6% of net primary production of the watershed was lost as aquatic carbon emission, suggesting the aquatic carbon emission affected the agricultural-dominated watershed carbon balance. The river network acted as significant CO_2 and CH_4 sources with estimated emission fluxes of 409 ± 365 mmol m^{-2} d^{-1} for CO_2 and 1.6 ± 1.2 mmol m^{-2} d^{-1} for CH_4, and dominated the total aquatic diffusion carbon emission of the watershed.

CRediT authorship contribution statement

Qitao Xiao: Conceptualization, Methodology, Investigation, Formal analysis, Writing – original draft, Writing – review & editing. **Zhenghua Hu:** Methodology, Writing – review & editing, Supervision, Funding acquisition. **Cheng Hu:** Formal analysis, Writing – review & editing. **A.R.M. Towfiqul Islam:** Formal analysis, Writing – review & editing. **Hang Bian:** Investigation, Formal analysis. **Shutao Chen:** Conceptualization, Resources. **Chao Liu:** Investigation. **Xuhui Lee:** Conceptualization.

Declaration of competing interest

The authors declare that they have no known competing financial interests or personal relationships that could have appeared to influence the work reported in this paper.

Acknowledgements

This study was funded jointly by the National Natural Science Foundation of China (41801093, 41775152, and 41775151). We would like to thank all participants of the Yale-NUIST Center on Atmospheric Environment for their help with sample collection, field measurements, and data analysis.

Appendix A. Supplementary data

Supplementary data to this article can be found online at https://doi.org/10.1016/j.scitotenv.2020.144558.

References

Abril, G., Martinez, J.M., Artigas, L.F., Moreira-Turcq, P., Benedetti, M.F., Vidal, L., Meziane, T., Kim, J.H., Bernardes, M.C., Savoye, N., Deborde, J., Souza, E.L., Alberic, P., Landim de Souza, M.F., Roland, F., 2014. Amazon River carbon dioxide outgassing fuelled by wetlands. Nature 505, 395–398.

Audet, J., Wallin, M.B., Kyllmar, K., Andersson, S., Bishop, K., 2017. Nitrous oxide emissions from streams in a Swedish agricultural catchment. Agric. Ecosyst. Environ. 236, 295–303.

Aufdenkampe, A.K., Mayorga, E., Raymond, P.A., Melack, J.M., Doney, S.C., Alin, S.R., Aalto, R.E., Yoo, K., 2011. Riverine coupling of biogeochemical cycles between land, oceans, and atmosphere. Front. Ecol. Environ. 9, 53–60.

Bastviken, D., Tranvik, L.J., Downing, J.A., Crill, P.M., Enrich-Prast, A., 2011. Freshwater methane emissions offset the continental carbon sink. Science 331 50–50.

Beaulieu, J.J., DelSontro, T., Downing, J.A., 2019. Eutrophication will increase methane emissions from lakes and impoundments during the 21st century. Nat. Commun. 10, 1375.

Bodmer, P., Heinz, M., Pusch, M., Singer, G., Premke, K., 2016. Carbon dynamics and their link to dissolved organic matter quality across contrasting stream ecosystems. Sci. Total Environ. 553, 574–586.

Borges, A.V., Darchambeau, F., Teodoru, C.R., Marwick, T.R., Tamooh, F., Geeraert, N., Omengo, F.O., Guérin, F., Lambert, T., Morana, C., 2015. Globally significant greenhouse-gas emissions from African inland waters. Nat. Geosci. 8, 637–642.

Borges, A.V., Darchambeau, F., Lambert, T., Bouillon, S., Morana, C., Brouyere, S., Hakoun, V., Jurado, A., Tseng, H.C., Descy, J.P., Roland, F.A., 2018. Effects of agricultural land use on fluvial carbon dioxide, methane and nitrous oxide concentrations in a large European river, the Meuse (Belgium). Sci. Total Environ. 610, 342–355.

Borges, A.V., Darchambeau, F., Lambert, T., Morana, C., Allen, G., Tambwe, E., Sembatio, A., Mambo, T., Wabakhangazi, J., Descy, J., Teodoru, C., Bouillon, S., 2019. Variations in dissolved greenhouse gases (CO_2, CH_4, N_2O) in the Congo River network overwhelmingly driven by fluvial-wetland connectivity. Biogeosciences 16, 3801–3834.

Butman, D., Raymond, P.A., 2011. Significant efflux of carbon dioxide from streams and rivers in the United States. Nat. Geosci. 4, 839–842.

Butman, D., Stackpoole, S., Stets, E., McDonald, C.P., Clow, D.W., Striegl, R.G., 2016. Aquatic carbon cycling in the conterminous United States and implications for terrestrial carbon accounting. Proc. Natl. Acad. Sci. U. S. A. 113, 58–63.

Campeau, A., Del Giorgio, P.A., 2014. Patterns in CH_4 and CO_2 concentrations across boreal rivers: major drivers and implications for fluvial greenhouse emissions under climate change scenarios. Glob. Chang. Biol. 20, 1075–1088.

Clough, T.J., Buckthought, L.E., Kelliher, F.M., Sherlock, R.R., 2007. Diurnal fluctuations of dissolved nitrous oxide (N_2O) concentrations and estimates of N_2O emissions from a spring-fed river: implications for IPCC methodology. Glob. Chang. Biol. 13, 1016–1027.

Cole, J.J., Caraco, N.F., 1998. Atmospheric exchange of carbon dioxide in a low-wind oligotrophic lake measured by the addition of SF_6. Limnol. Oceanogr. 43, 647–656.

Cole, J.J., Prairie, Y.T., Caraco, N.F., McDowell, W.H., Tranvik, L.J., Striegl, R.G., Duarte, C.M., Kortelainen, P., Downing, J.A., Middelburg, J.J., Melack, J., 2007. Plumbing the global carbon cycle: integrating inland waters into the terrestrial carbon budget. Ecosystems 10, 171–184.

Crawford, J.T., Stanley, E.H., 2016. Controls on methane concentrations and fluxes in streams draining human-dominated landscapes. Ecol. Appl. 26, 1581–1591.

Deemer, B.R., Harrison, J.A., Li, S., Beaulieu, J.J., DelSontro, T., Barros, N., Bezerra-Neto, J.F., Powers, S.M., dos Santos, M.A., Vonk, J.A., 2016. Greenhouse gas emissions from reservoirwater surfaces: a new global synthesis. BioScience 66, 949–964.

Dinsmore, K.J., Billett, M.F., Dyson, K.E., 2013. Temperature and precipitation drive temporal variability in aquatic carbon and GHG concentrations and fluxes in a peatland catchment. Glob. Chang. Biol. 19, 2133–2148.

Duvert, C., Butman, D.E., Marx, A., Ribolzi, O., Hutley, L.B., 2018. CO_2 evasion along streams driven by groundwater inputs and geomorphic controls. Nat. Geosci. 11, 813–818.

Foley, J.A., DeFries, R., Asner, G.P., Barford, C., Bonan, G., Carpenter, S.R., Chapin, F.S., Coe, M.T., Daily, G.C., Gibbs, H.K., Helkowski, J.H., Holloway, T., Howard, E.A., Kucharik, C.J., Monfreda, C., Patz, J.A., Prentice, I.C., Ramankutty, N., Snyder, P.K., 2005. Global consequences of land use. Science 309, 570–574.

Fu, C., Lee, X., Griffis, T., Baker, J., Turner, P., 2018. A modeling study of direct and indirect N_2O emissions from a representative catchment in the U.S. Corn Belt. Water Resour. Res. 54, 3632–3653.

Garnier, J., Vilain, G., Silvestre, M., Billen, G., Jehanno, S., Poirier, D., Martinez, A., Decuq, C., Cellier, P., Abril, G., 2013. Budget of methane emissions from soils, livestock and the river network at the regional scale of the seine basin (France). Biogeochemistry 116, 199–214.

Griffis, T.J., Chen, Z., Baker, J.M., Wood, J.D., Millet, D.B., Lee, X., Venterea, R.T., Turner, P.A., 2017. Nitrous oxide emissions are enhanced in a warmer and wetter world. Proc. Natl. Acad. Sci. U. S. A. 114, 12081–12085.

Holgerson, M.A., Raymond, P.A., 2016. Large contribution to inland water CO_2 and CH_4 emissions from very small ponds. Nat. Geosci. 9, 222–226.

Hu, B., Wang, D., Zhou, J., Meng, W., Li, C., Sun, Z., Guo, X., Wang, Z., 2018. Greenhouse gases emission from the sewage draining rivers. Sci. Total Environ. 612, 1454–1462.

Humborg, C., Morth, C.M., Sundbom, M., Borg, H., Blenckner, T., Giesler, R., Ittekkot, V., 2010. CO_2 supersaturation along the aquatic conduit in Swedish watersheds as constrained by terrestrial respiration, aquatic respiration and weathering. Glob. Chang. Biol. 16, 1966–1978.

Huotari, J., Nykanen, H., Forsius, M., Arvola, L., 2013. Effect of catchment characteristics on aquatic carbon export from a boreal catchment and its importance in regional carbon cycling. Glob. Chang. Biol. 19, 3607–3620.

Kirschke, S., Bousquet, P., Ciais, P., Saunois, M., Canadell, J.G., Dlugokencky, E.J., Bergamaschi, P., Bergmann, D., Blake, D.R., Bruhwiler, L., Cameron-Smith, P., Castaldi, S., Chevallier, F., Feng, L., Fraser, A., Heimann, M., Hodson, E.L., Houweling, S., Josse, B., Fraser, P.J., Krummel, P.B., Lamarque, J.F., Langenfelds, R.L., Le Quéré, C., Naik, V., O'Doherty, S., Palmer, P.I., Pison, I., Plummer, D., Poulter, B., Prinn, R.G., Rigby, M., Ringeval, B., Santini, M., Schmidt, M., Shindell, D.T., Simpson, I.J., Spahni, R., Steele, L.P., Strode, S.A., Sudo, K., Szopa, S., van der Werf, G.R., Voulgarakis, A.,

van Weele, M., Weiss, R.F., Williams, J.E., Zeng, G., 2013. Three decades of global methane sources and sinks. Nat. Geosci. 6, 813–823.
Kortelainen, P., Rantakari, M., Huttunen, J.T., Mattsson, T., Alm, J., Juutinen, S., Larmola, T., Silvola, J., Martikainen, P.J., 2006. Sediment respiration and lake trophic state are important predictors of large CO_2 evasion from small boreal lakes. Glob. Chang. Biol. 12, 1554–1567.
Lauerwald, R., Laruelle, G.G., Hartmann, J., Ciais, P., Regnier, P.A., 2015. Spatial patterns in CO_2 evasion from the global river network. Glob. Biogeochem. Cycles 29, 534–554.
Li, S., Bush, R.T., Santos, I.R., Zhang, Q., Song, K., Mao, R., Wen, Z., Lu, X.X., 2018. Large greenhouse gases emissions from China's lakes and reservoirs. Water Res. 147, 13–24.
Li, S., Mao, R., Ma, Y., Sarma, V., 2019. Gas transfer velocities of CO_2 in subtropical monsoonal climate streams and small rivers. Biogeosciences 16, 681–693.
Li, X.B., Xia, Y.Q., Li, Y.F., Kana, T.M., Kimura, S.D., Saito, M., Yan, X.Y., 2013. Sediment denitrification in waterways in a rice-paddy-dominated watershed in eastern China. J. Soils Sediments 13, 783–792.
Ma, Y., Sun, L., Liu, C., Yang, X., Zhou, W., Yang, B., Schwenke, G., Liu, L., 2018. A comparison of methane and nitrous oxide emissions from inland mixed-fish and crab aquaculture ponds. Sci. Total Environ. 637-638, 517–523.
Maberly, S.C., Barker, P.A., Stott, A.W., De Ville, M.M., 2013. Catchment productivity controls CO_2 emissions from lakes. Nat. Clim. Chang. 3, 391–394.
Morales-Williams, A.M., Wanamaker, A.D., Williams, C.J., Downing, J.A., 2020. Eutrophication drives extreme seasonal CO_2 flux in lake ecosystems. Ecosystems https://doi.org/10.1007/s10021-020-00527-2.
Ollivier, Q.R., Maher, D.T., Pitfield, C., Macreadie, P.I., 2019. Punching above their weight: large release of greenhouse gases from small agricultural dams. Glob. Chang. Biol. 25, 721–732.
Qin, B., Xu, P., Wu, Q., Luo, L., Zhang, Y., 2007. Environmental issues of Lake Taihu, China. Hydrobiologia 581, 3–14.
Raymond, P.A., Hartmann, J., Lauerwald, R., Sobek, S., McDonald, C., Hoover, M., Butman, D., Striegl, R., Mayorga, E., Humborg, C., Kortelainen, P., Durr, H., Meybeck, M., Ciais, P., Guth, P., 2013. Global carbon dioxide emissions from inland waters. Nature 503, 355–359.
Richey, J.E., Melack, J.M., Aufdenkampe, A.K., Ballester, V.M., Hess, L.L., 2002. Outgassing from Amazonian rivers and wetlands as a large tropical source of atmospheric CO_2. Nature 416, 617–620.
Schrier-Uijl, A.P., Veraart, A.J., Leffelaar, P.A., Berendse, F., Veenendaal, E.M., 2011. Release of CO_2 and CH_4 from lakes and drainage ditches in temperate wetlands. Biogeochemistry 102, 265–279.
Sinha, E., Michalak, A.M., Balaji, V., 2017. Eutrophication will increase during the 21st century as a result of precipitation changes. Science 357, 405–408.
Smith, R., Kaushal, S., Beaulieu, J., Pennino, M., Welty, C., 2017. Influence of infrastructure on water quality and greenhouse gas dynamics in urban streams. Biogeosciences 14, 2831–2849.
Stanley, E.H., Casson, N.J., Christel, S.T., Crawford, J.T., Loken, L.C., Oliver, S.K., 2016. The ecology of methane in streams and rivers: patterns, controls, and global significance. Ecol. Monogr. 86, 146–171.
Striegl, R.G., Dornblaser, M.M., McDonald, C.P., Rover, J.R., Stets, E.G., 2012. Carbon dioxide and methane emissions from the Yukon River system. Global Biogeochemical Cycles 26, GB0E05.
Wang, X., He, Y., Yuan, X., Chen, H., Peng, C., Zhu, Q., Yue, J., Ren, H., Deng, W., Liu, H., 2017. pCO_2 and CO_2 fluxes of the metropolitan river network in relation to the urbanization of Chongqing, China. Journal of Geophysical Research-Biogeosciences 122, 470–486.
Wanninkhof, R., 1992. Relationship between wind speed and gas exchange over the ocean. J. Geophys. Res. 97, 7373–7382.
Wu, S., Li, S., Zou, Z., Hu, T., Hu, Z., Liu, S., Zou, J., 2019. High methane emissions largely attributed to ebullitive fluxes from a subtropical river draining a rice paddy watershed in China. Environ. Sci. Technol. 53, 3499–3507.
Xia, Y.Q., Li, Y.F., Ti, C.P., Li, X.B., Zhao, Y.Q., Yan, X.Y., 2013. Is indirect N_2O emission a significant contributor to the agricultural greenhouse gas budget? A case study of a rice paddy-dominated agricultural watershed in eastern China. Atmos. Environ. 77, 943–950.
Xiao, Q., Zhang, M., Hu, Z., Gao, Y., Hu, C., Liu, C., Liu, S., Zhang, Z., Zhao, J., Xiao, W., Lee, X., 2017. Spatial variations of methane emission in a large shallow eutrophic lake in subtropical climate. Journal of Geophysical Research-Biogeosciences 122, 1597–1614.
Xiao, Q., Hu, Z., Fu, C., Bian, H., Lee, X., Chen, S., Shang, D., 2019a. Surface nitrous oxide concentrations and fluxes from water bodies of the agricultural watershed in eastern China. Environ. Pollut. 251, 185–192.
Xiao, Q., Xu, X., Zhang, M., Duan, H., Hu, Z., Wang, W., Xiao, W., Lee, X., 2019b. Coregulation of nitrous oxide emissions by nitrogen and temperature in China's third largest freshwater Lake (Lake Taihu). Limnol. Oceanogr. 64, 1070–1086.
Xiao, Q., Xu, X., Duan, H., Qi, T., Qin, B., Lee Xu, Hu Z., Wang, W., Xiao, W., Zhang, M., 2020. Eutrophic Lake Taihu as a significant CO_2 source during 2000-2015. Water Res. 170, 115331.
Xu, X., Yang, G., Tan, Y., Tang, X., Jiang, H., Sun, X., Zhuang, Q., Li, H., 2017. Impacts of land use changes on net ecosystem production in the Taihu Lake Basin of China from 1985 to 2010. Journal of Geophysical Research-Biogeosciences 122, 690–707.
Yan, X., Cai, Z., Yang, R., Ti, C., Xia, Y., Li, F., Wang, J., Ma, A., 2011. Nitrogen budget and riverine nitrogen output in a rice paddy dominated agricultural watershed in eastern China. Biogeochemistry 106, 489–501.
Yang, P., Zhang, Y., Lai, D.Y., Tan, L., Jin, B., Tong, C., 2018. Fluxes of carbon dioxide and methane across the water-atmosphere interface of aquaculture shrimp ponds in two subtropical estuaries: the effect of temperature, substrate, salinity and nitrate. Sci. Total Environ. 635, 1025–1035.
Yang, P., Zhang, Y., Yang, H., Zhang, Y., Xu, J., Tan, L., Tong, C., Lai, D.Y., 2019. Large fine-scale spatiotemporal variations of CH_4 diffusive fluxes from shrimp aquaculture ponds affected by organic matter supply and aeration in Southeast China. Journal of Geophysical Research-Biogeosciences 124, 1290–1307.
Yu, Z., Wang, D., Li, Y., Deng, H., Hu, B., Ye, M., Zhou, X., Da, L., Chen, Z., Xu, S., 2017. Carbon dioxide and methane dynamics in a human-dominated lowland coastal river network (Shanghai, China). Journal of Geophysical Research-Biogeosciences 122, 1738–1758.
Yvon-Durocher, G., Allen, A.P., Bastviken, D., Conrad, R., Gudasz, C., St-Pierre, A., Thanh-Duc, N., del Giorgio, P.A., 2014. Methane fluxes show consistent temperature dependence across microbial to ecosystem scales. Nature 507, 488–491.
Raymond, P.A., Zappa, C.J., Butman, D., Bott, T.L., Potter, J., Mulholland, P., Laursen, A.E., Mcdowell, W.H., Newbold, D., 2012. Scaling the gas transfer velocity and hydraulic geometry in streams and small rivers. Limnology Oceanography Fluids Environment 2, 41–53.
Zhang, W., Li, H., Xiao, Q., Jiang, S., Li, X., 2020. Surface nitrous oxide (N_2O) concentrations and fluxes from different rivers draining contrasting landscapes: Spatio-temporal variability, controls, and implications based on IPCC emission factor. Environ. Pollut. 263, 114457.
Zhao, Y., Xia, Y., Kana, T., Wu, Y., Li, X., Yan, X., 2013. Seasonal variation and controlling factors of anaerobic ammonium oxidation in freshwater river sediments in the Taihu Lake region of China. Chemosphere 93, 2124–2131.
Zhou, W., Lin, J., Tang, Q., Wei, Z., Schwenke, G., Liu, D.L., Yan, X., 2019. Indirect N_2O emissions from groundwater under high nitrogen-load farmland in eastern China. Environ. Pollut. 248, 238–246.